RESEARCH

Forced internal desynchrony induces cardiometabolic alterations in adult rats

Isis Gabrielli Barbieri de Oliveira[1], Marcos Divino Ferreira Junior[1], Paulo Ricardo Lopes[1], Dhiogenes Balsanufo Taveira Campos[1], Marcos Luiz Ferreira-Neto[2], Eduardo Henrique Rosa Santos[2], Paulo Cezar de Freitas Mathias[3], Flávio Andrade Francisco[3], Bruna Del Vechio Koike[4], Carlos Henrique de Castro[5], André Henrique Freiria-Oliveira[1], Gustavo Rodrigues Pedrino[1], Rodrigo Mello Gomes[1] and **Daniel Alves Rosa[1]**

[1]Center of Neuroscience and Cardiovascular Research, Biological Science Institute, Federal University of Goiás, Goiânia, Goiás, Brazil
[2]Departament of Physiology, Institute of Biomedical Science, Laboratory of Electrophysiology and Cardiovascular Physiology, Federal University of Uberlândia, Uberlândia, Minas Gerais, Brazil
[3]Department of Biotechnology, Genetics and Cell Biology, Laboratory of Secretion Cell Biology, State University of Maringá, Maringá, Paraná, Brazil
[4]Medical Department, Federal University of San Francisco Valley, Petrolina, Pernambuco, Brazil
[5]Department of Physiological Science, Integrative Laboratory of Cardiovascular and Neurological Pathophysiology, Biological Science Institute, Federal University of Goiás, Goiânia, Goiás, Brazil

Correspondence should be addressed to D A Rosa: danielr@ufg.br

Abstract

Disruptions in circadian rhythms have been associated with several diseases, including cardiovascular and metabolic disorders. Forced internal desynchronization induced by a period of T-cycles of 22 h (T22 protocol) reaches the lower limit of entrainment and dissociates the circadian rhythmicity of the locomotor activity into two components, driven by different outputs from the suprachiasmatic nucleus (SCN). The main goal of this study was to evaluate the cardiovascular and metabolic response in rats submitted to internal desynchronization by T22 protocol. Male Wistar rats were assigned to either a control group subjected to a usual T-cycles of 24 h (12 h–12 h) or an experimental group subjected to the T22 protocol involving a 22-h symmetric light–dark cycle (11 h–11 h). After 8 weeks, rats subjected to the T22 exhibited desynchrony in their locomotor activity. Although plasma glucose and insulin levels were similar in both groups, desynchronized rats demonstrated dyslipidemia, significant hypertrophy of the fasciculate zone of the adrenal gland, low IRB, IRS2, PI3K, AKT, SOD and CAT protein expression and an increased expression of phosphoenolpyruvate carboxykinase in the liver. Furthermore, though they maintained normal baseline heart rates and mean arterial pressure levels, they also presented reduced baroreflex sensitivity. The findings indicate that circadian timing desynchrony following the T22 protocol can induce cardiometabolic disruptions. Early hepatic metabolism dysfunction can trigger other disorders, though additional studies are needed to clarify the causes.

Key Words

- insulin resistance
- circadian rhythms
- metabolism
- blood pressure
- corticosteroids

Journal of Endocrinology (2019) **242**, 25–36

Introduction

In mammals, the circadian timing system comprises a central oscillator in the hypothalamic suprachiasmatic nucleus (SCN) containing autonomous single cells, which cause circadian oscillation, and peripheral oscillators, including muscle and adipose tissue, the pancreas and the liver (Inouye & Kawamura 1979, Diez-Noguera *et al.* 1994, Mohawk & Takahashi 2011). The SCN not only transduces information about environmental light–dark

https://joe.bioscientifica.com
https://doi.org/10.1530/JOE-19-0026

cycles but also receives external and internal time cues, including changes in light intensity, from the retina and bodily substance levels. Consequently, the SCN can synchronize changes in environmental light with the daily rhythm of various biological and behavioral components, including body temperature, hormones release and sleep–wake cycles (Coomans *et al.* 2015, Kingsbury *et al.* 2016). Meanwhile, peripheral cells in the heart, liver and pancreas also contain intrinsic circadian oscillators (Pezuk *et al.* 2010, Podobed *et al.* 2014). These peripheral oscillators maintain their period and phase rhythms of cellular activity when assessed in isolation, although central SCN pacemaker cells are probably needed to synchronize temporal physiology in the whole organism (Gachon *et al.* 2004, Richards *et al.* 2013). The lack of synchrony between oscillators, however, can cause health problems, including ones associated with jet lag, shift work and poor sleep quality (Casiraghi *et al.* 2012, 2016, Golombek *et al.* 2013, Cudney *et al.* 2014, Laing *et al.* 2015, Oike *et al.* 2015). Altogether, the SCN is the master clock primarily responsible for maintaining phase coherence within the body's complex network of oscillators.

In the mammalian cardiovascular system, circadian rhythms is present in several physiological parameters, including blood pressure (BP), heart rate (HR) and cardiac contractility (Bray *et al.* 2008, Denniff *et al.* 2014, Portaluppi 2014, Alibhai *et al.* 2015). Furthermore, clock mutant mice Clock$^{\Delta 19/\Delta 19}$ (King *et al.* 1997, Gekakis 1998), known to showing locomotor activity disrupt, can also typically show development of cardiac disturbances, including increased heart weight, cardiomyocyte hypertrophy, interstitial fibrosis and cardiac malfunction (Alibhai *et al.* 2017). At the same time, hormones such as insulin and cortisol present circadian rhythmicity (Tseng *et al.* 2015). The glucocorticoids are released from the adrenal gland in a rhythmic mode under normal circadian rhythm conditions, and its daily peak is associated with the onset of the activity period, preparing the body by inducing catabolic reactions of energy stores (Kalsbeek *et al.* 2012, Bedrosian *et al.* 2016).

In clinical and experimental studies, researchers have demonstrated that the altered expression of circadian clock genes relates to metabolic syndrome (Gómez-Abellán *et al.* 2008, Scott *et al.* 2008). As a result, the disruption of the circadian system and increased corticosterone levels relate to increased adiposity and the development of other parameters of metabolic syndrome (Báez-Ruiz *et al.* 2017). Although many evidence suggests that the desynchronization of circadian rhythm increases the risk of cardiometabolic disorders (Scheer *et al.* 2009, Karatsoreos *et al.* 2011, Morris *et al.* 2012, 2016, 2018, Golombek *et al.* 2013, Ben-Hamo *et al.* 2016, West *et al.* 2017), new experimental approaches are needed to understand the phenomenon.

Models for studying circadian desynchrony are pivotal to understanding the mechanisms affected by biological rhythms. Campuzano *et al.* (1998) developed a forced desynchronization of locomotor activity rhythm, a so-called 'internal forced desynchronization protocol (T22)' involves subjecting rats to a symmetric 22-h light–dark cycle (11:11LD). Those authors observed that rats subjected to the light–dark cycle at the limit of synchronization period T-cycles of 22 h expressed two rhythmic components of spontaneous locomotor activity simultaneously with different periods (Campuzano *et al.* 1998). Such results suggest that dissociating circadian rhythms by implementing the T22 protocol can aid pathophysiological investigations into circadian rhythm disorders. Indeed, rats submitted to the protocol have presented primary features found in forced desynchronization in humans, including the altered circadian regulation of temperature, sleep architecture and melatonin and cortisol secretion (Cambras *et al.* 2007, Schwartz *et al.* 2009, Wotus *et al.* 2013, Casiraghi *et al.* 2016).

Nevertheless, many mechanisms involved in those condition and their effects are not fully understood, as do the effects of implementing the T22 protocol on cardiovascular and metabolic outcomes. Here, we hypothesized that the desynchronization of circadian rhythm could be a risk factor of the onset of cardiometabolic disorders associated with disruptions of the hypothalamic–pituitary–adrenal axis and liver metabolism. In this way, we investigated the effects of the T22 protocol on baseline mean arterial pressure (MAP), HR, the sensibility of the baroreceptor reflex and metabolic parameters, including insulin signaling in the liver and adrenal gland morphology.

Materials and methods

Animals

All experimental protocols were performed in accordance with the guidelines of the National Council of Animal Experiments Control (CONCEA) and approved by the Ethics Committee on the Use of Animals of the Federal University of Goiás, Goiânia, Brazil (protocol no. 091/15).

https://joe.bioscientifica.com
https://doi.org/10.1530/JOE-19-0026

Male Wistar rats 60 days old weighing 250–300 g from the Central Animal Facility of the Federal University of Goiás were housed in the Animal Facility of the Department of Physiological Sciences of the Federal University of Goiás in standard polypropylene cages (30 × 20 × 13 cm^3) and given free access to water and standard nonpurified rodent chow (Nuvilab, Colombo, PR, Brazil). Cages were placed in an animal facility with controlled temperature (22 ± 2°C) and humidity (55 ± 10%). Initially, all animals were kept under inverted 12-h–12-h light–darkness cycle – lights on at 18:00 h – for 1 week before experiments commenced. Each animal was randomly assigned to one of two photoperiod conditions for 8 weeks; control animals (CTR, $n = 13$) were singly housed under a 24-h light–dark cycle (12 h–12 h), whereas desynchronized animals (DSC, $n = 19$) were subjected to a T22 protocol consisting of a 22-h symmetric light–darkness cycle (11 h–11 h). In all cases, light consisted of 200 lx during the light phase and at time of lights on a defined Zeitgeber time 0 (ZT0). Throughout the protocol period, all animals were weighted and recorded their food intake once a week. The weight and area under de curve (AUC) of the food intake were used to compare both groups in the end of protocol.

Locomotor activity analysis

Spontaneous locomotor activity was continuously monitored using infrared motion sensors (DYP-ME003 PIR Motion Sensor Module) placed 15 cm above cages, and data were recorded every 5 min by a software system (SAP-LNRB, developed by Dr Marconi Camara Rodrigues, Universidade Federal do Rio Grande do Norte, Natal, RN, Brazil). Actograms and rhythm analysis were performed with El Temps software (Díez-Noguera, Universitat de Barcelona, Barcelona, Spain). The period of locomotor activity was assessed via periodogram analysis, as described by Sokolove & Bushell (1978), and internal desynchronization was confirmed by two locomotor rhythmic components expressed in periods of different lengths. Rats not exhibiting relative desynchronization were removed from experiments. For all animals, totals and percentages of locomotor activity in each phase of the light–dark cycle were calculated as the sum of locomotor activity obtained by each animal during the protocol.

Euthanasia and sample collection

After the experimental period, animals fasted for 12 h, were anesthetized with thiopental sodium (45 mg/kg of BW, i.p., Thiopentax, Cristália, Itapira, SP, Brazil), and killed by exsanguination for the collection of blood, liver and adrenal gland samples. Blood samples were centrifuged at 120 ***g*** for 15 min for plasma collection and stored at −20°C for subsequent analyses. All animals were killed during the mid-dark phase of their light–dark cycle: ZT18 for CTR animals and ZT16–17 for DSC animals.

Biochemical and hormonal analyses

Blood samples were used to measure blood glucose (Gold Analisa Belo Horizonte, MG, Brazil) triglycerides, total cholesterol, high-density lipoprotein (HDL) cholesterol by enzymatic colorimetric methods according to the manufacturer's instructions (de Oliveira *et al.* 2018). Low-density lipoprotein (LDL) and very LDL cholesterols were calculated according to the Friedewald equation (LDL = total cholesterol − (HDL + VLDL); VLDL = triglycerides/5). To calculate Castelli indexes I and II, the formulas of (Fagundes *et al.* 2009) were used (Castelli index I = total cholesterol/HDL cholesterol; Castelli index II = LDL cholesterol/HDL cholesterol). Plasma insulin was measured by radioimmunoassay in a gamma counter (Wizard2 Automatic Gamma Counter, TM-2470, PerkinElmer) using standard human insulin and anti-rat insulin antibodies (Sigma–Aldrich) and recombinant human insulin labeled Iodo125 (PerkinElmer). Intra-assay coefficients of variation ranged from 8 to 10%; the limit of detection was 0.006 ng/mL.

Adrenal gland morphometric analyses

Adrenal gland samples were removed and fixed in 10% formalin and embedded in paraffin (BIOTEC, Pinhais, PR, Brazil), and nonserial histological sections 6 µm thick were cut with a Leica RM2145 semimotorized rotary microtome (Leica RM2155, Leica Microsystems) and stained with hematoxylin and eosin. Morphometric analyses were performed using digital images (TIFF 24-bit color, 2560 × 1920 pixels) obtained with a light microscope (Leica DM500, Leica Microsystems) and digital image acquisition system (Leica Application Suite, V.3.10, Leica Microsystems). Quantitative analysis of total adrenal area was performed using digital images (20× magnification) from five fields from each animal ($n = 6$ animals/group), whereas analyses of the adrenal medullary, cortex and zona fasciculata areas were separately performed using digital images (200× magnification) from ten fields from each animal ($n = 6$ animals/group). Total cell nuclei were counted using digital images (1000× magnification) in a

https://joe.bioscientifica.com
https://doi.org/10.1530/JOE-19-0026

defined area from ten random fields in the zona fasciculata from six animals per group, and cell nuclei per μm² were calculated as the total number of nuclei in ten defined areas divided by total area. Analyses were performed using Image J 1.34s software (National Institutes of Health).

Western blotting

Liver samples were homogenized in cold lysis buffer (50 mM Hepes, pH 6.4, 1 mM $MgCl_2$, 10 mM EDTA and 1% Triton X-100) containing protease inhibitors (10 μg/μL aprotinin, 10 μg/μL leupeptin, 2 μg/μL pepstatin, and 1 mM phenylmethylsufonic fluoride; Sigma–Aldrich) using a homogenizer (Ultra-Turrax, IKA Werke, Staufen, Germany). After centrifugation, homogenates were stored at −20°C. Protein concentration in the supernatant was determined with a Pierce BCA Protein Assay Kit (Thermo Fisher Scientific). Once the supernatant was resuspended in Laemmli sample buffer and boiled at 95°C for 5 min, samples (30 μg of total protein) were separated by polyacrylamide gel electrophoresis in 10–12% Tris-glycine SDS polyacrylamide gels. Proteins were transferred to PVDF membranes (Hybond ECL; Amersham Pharmacia Biotech, London, UK), blocked in 5% dry milk in Tween 20 Tris-buffered saline (T-TBS; 0.02 M Tris/0.15 M NaCl, pH 7.5 containing 0.1% Tween 20) at room temperature for 1 h, washed 3 times with T-TBS and incubated with the primary antibodies (insulin pathway: IRB, IRS2, PI3K and AKT; gluconeogenic enzyme: phosphoenolpyruvate carboxykinase (PEPCK); antioxidant defense: SOD and CAT at 1:500 concentration; Santa Cruz Biotechnology) overnight at 4°C. Membranes were washed and incubated for 120 min at room temperature with specific HRP-conjugated secondary antibody diluted to 1:2,000 (goat anti-mouse IgGHRP: sc-2005; goat anti-rabbit IgGHRP: sc-2004, both from Santa Cruz Biotechnology). Proteins recognized by the secondary antibodies were detected by chemiluminescence (Amersham ECL Prime, GE), and the blot was visualized on ImageQuant LAS 500 (GE Healthcare Life Sciences). Band intensities were quantified by optical densitometry using Image J software (National Institutes of Health). Band intensities were normalized to those of total protein or loading control (beta actin or GAPDH), and results were expressed as relative (%) to the control group.

Measurement of cardiovascular parameters

After the experimental period, another subgroup of animals from both groups were anesthetized intraperitoneally with a mixture of ketamine (70 mg/kg; Sespo, Paulínia, SP, Brazil) and xylazine (30 mg/kg; Rhobifarma, Hortolândia, SP, Brazil) and polyethylene catheters (PE10) were inserted into the abdominal aorta via the femoral artery and vein, both exteriorized at the neck, to record arterial pressure and drug injections, respectively. After cannulation, two subcutaneous bipolar electrodes were implanted dorsally to record HR and the bipolar lead D2 of the electrocardiogram. Pentabiotic (200 mg/kg; Fort Dodge Saúde Animal, Campinas, Brazil) and 1.0 mg/kg of flunixin (Chemitec, São Paulo, Brazil) were administered intramuscularly to prevent infection and pain. MAP, pulsatile arterial pressure (PAP), and HR were recorded in freely moving rats at least 24 h after surgery and during the mid-dark phase of the light–dark cycle. Data were recorded continuously by a PowerLab System Device, and data acquisition was performed with LabChart 8 for Windows (ADInstruments, New South Wales, Australia).

Baroreflex test

After baseline recordings of 30 min of MAP and HR, animals received an intravenous bolus injection of three random doses of phenylephrine (1 μg, 2.5 μg and 5 μg; Sigma–Aldrich) or sodium nitroprusside (5 μg, 10 μg and 20 μg; Sigma–Aldrich) to evaluate baroreflex sensitivity. The difference between the baseline 30 s before baroreflex activation or deactivation and the peak of all changes in MAP and HR produced by baroreflex activation or deactivation were measured as ΔMAP and ΔHR, respectively. The baroreflex index was evaluated by dividing the maximum ΔHR by the maximum ΔMAP produced by pressor (bradycardic index) or depressor (tachycardia index) drugs. The quantitative measure of the baroreceptor sensitivity was averaged in terms of the ΔHR:ΔMAP ratio.

Statistical analysis

Data were processed as mean ± S.E.M. Statistical analyses were performed using an unpaired Student's *t* test when CTR vs DSC groups were compared for nearly all parameters. Two-way ANOVA following *post hoc* Bonferroni's test was performed only for the percentage of locomotor activity during light and dark phases of the light–dark cycle. Differences were considered significant at $P<0.05$. Statistical analysis and graphs were performed using GraphPad Prism version 6.0 software for Windows (GraphPad Software Inc.).

https://joe.bioscientifica.com
https://doi.org/10.1530/JOE-19-0026

Results

Effect of circadian desynchrony on locomotor activity

Figure 1 shows representative images of the rest–activity cycle plotted as actograms demonstrating the circadian rhythm of the locomotor activity of CTR and DSC animals (Fig. 1A). Periodogram analysis revealed that rats submitted to a T22 protocol presented desynchrony in locomotor activity rhythm, which prompted one component aligned with the light–dark cycle (22-h period) and another with 24.8±0.05 h, thereby showing a free run period of the rest–activity cycle (Fig. 1B). Total locomotor activity did not significantly differ between the groups (CTR 550.6±60.3 a.u. vs DSC 447.9±33.1 a.u.; $P=0.151$; Fig. 2A). However, DSC rats exhibited a greater percentage of locomotor activity during the light phase (CTR 9.8±0.8% vs DSC 26.5±0.7%; $P<0.001$; Fig. 2B) and a lower percentage during the dark phase (CTR 90.1±0.8% vs DSC 73.4±0.7%; $P<0.001$; Fig. 2B) than CTR rats.

Effect of circadian desynchrony on biometric and biochemical parameters

DSC rats did not significantly differ in body weight or AUC of food intake compared to CTR animals, nor in fasting blood glucose, insulin, total cholesterol and triglyceride levels (Table 1). However, LDL cholesterol was 51% greater and HDL cholesterol 31% less in DSC than that in CTR rats ($P<0.05$; Table 1). DSC rats also had 35 and 56% greater Castelli I and II indexes, respectively, than CTR rats ($P<0.05$; Table 1).

Effect of circadian desynchrony on adrenal gland morphology

Figure 3 illustrates the effect of circadian desynchrony induced by applying the T22 protocol on adrenal gland morphology. DSC rats showed a greater increase (42%) in adrenal gland mass than CTR rats (CTR 41.6±3.9 g vs DSC 59.2±3.7 mg; $P<0.01$; Fig. 3B). In addition, quantitative analysis revealed a significant increase (31%) in total adrenal gland area (CTR $5.5\times10^6\pm7.4\times10^5$ µm² vs DSC $7.3\times10^6\pm2.6\times10^5$ µm²; $P<0.01$; Fig. 3C) and significant hypertrophy of the cortical area (CTR $3.8\times10^6\pm1.8\times10^5$ µm² vs DSC $5.3\times10^6\pm1.9\times10^5$ µm²; $P<0.001$; Fig. 3E) in DSC rats compared to CTR rats, which indicates a greater zona fasciculata area (CTR $1.6\times10^6\pm5.8\times10^5$ µm² vs DSC $3.1\times10^6\pm3.8\times10^5$ µm²; $P<0.05$; Fig. 3F) and reduced number of nuclei per µm² therein (CTR 86.0±1.6 nuclei/µm² vs DSC 73.1±0.9 nuclei/µm²; $P<0.001$; Fig. 3G).

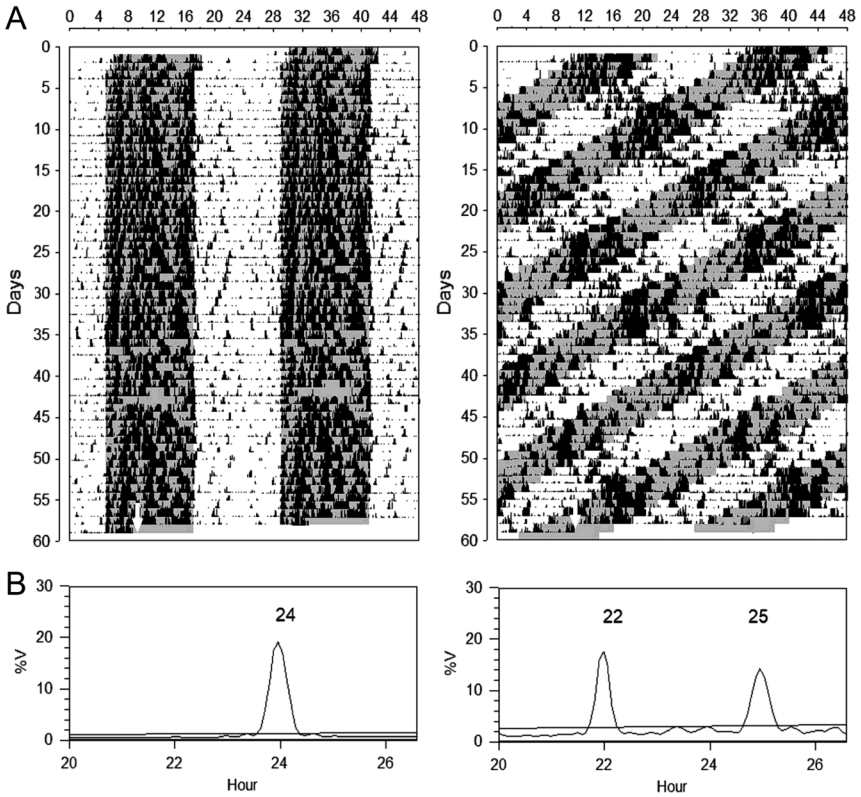

Figure 1
Graphs of representative spontaneous locomotor activity. (A) Double-plotted actograms of locomotor activity of representative rats maintained on a symmetric T24 h (left; 12 h–12 h light–dark) or T22 h cycle (right; 11 h–11 h light–dark). White arrow indicates the time of euthanasia for sample collection or cardiovascular test. (B) Sokolove–Bushell periodograms correspondent to the time series of each actogram. Analysis revealed a single peak at T24 h (left) for control animals (CTR) and two peaks for animals subjected to the desynchronization protocol (right, DSC); the first peak represents entrainment with the T22 h light–dark cycle, whereas the second one represents the period of free running for more than 24 h (representative rat = 25 h). %V = percentage of variance.

https://joe.bioscientifica.com
https://doi.org/10.1530/JOE-19-0026

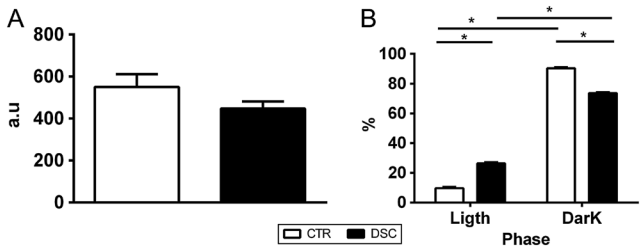

Figure 2
Effect of circadian rhythm desynchronization on locomotor activity. (A) Similar cumulative total amount of locomotor activity in rats in the control (CTR, $N = 13$, white bars) and desynchronized (DSC, $N = 19$, black bars) groups. (B) Percentage of locomotor activity during normal rest (light phase) and activity (dark phase) periods of the light–dark cycle. Both groups showed more activity during the dark than the light phase; however, DSC rats (black bars) showed higher locomotor activity during the light phase and lower locomotor activity during the dark phase than CTR rats (white bars) group. *$P < 0.05$ indicates a significant difference with an unpaired Student's *t* test or two-way ANOVA following by *post hoc* Bonferroni's test. a.u., arbitrary unit.

Nevertheless, adrenal medullary area did not differ between the groups (CTR $4.8 \times 10^5 \pm 3.6 \times 10^4$ µm² vs DSC $5.1 \times 10^5 \pm 3.4 \times 10^4$ µm²; $P = 0.6$; Fig. 3D).

Effect of circadian desynchrony on insulin signaling and PEPCK, SOD and CAT protein expression in the liver

Figure 4 illustrates the effect of circadian desynchrony on IRB, IRS2, PI3K and AKT expression in the liver. Hepatic IRB (CTR 100.0±3.6% of control vs DSC 55.5±5.9% of control; $P<0.01$; Fig. 4A), IRS2 (CTR 100.0±7.4% of control vs DSC 36.9±11.7% of control; $P<0.05$; Fig. 4B), PI3K (CTR 100.0±2.9% of control vs DSC 61.1±5.9% of control; $P<0.01$; Fig. 4C) and AKT (CTR 100.0±2.4% of control vs DSC 70.4±5.9% of control; $P<0.01$; Fig. 4D) expression was less in DSC rats than in CTR rats, whereas PEPCK expression was greater (CTR 100.0±27.3% of control vs DSC 211.0±11.1% of control; $P<0.05$; Fig. 5A). DSC rats also showed a lesser decrease in SOD (CTR 100.0±0.7% of control vs DSC 58.9±11.0% of control; $P<0.05$; Fig. 6A) and CAT (CTR 100.0±5.8% of control vs DSC 75.0±8.8% of control; $P<0.05$; Fig. 6B) expression in the liver than CTR animals did.

Table 1 Biometric and biochemical characterization of control (CTR) and desynchronized (DSC) rats.

	CTR ($n = 7$)	**DSC** ($n = 7$)
Body weight (g)	360.7 ± 17.1	354.3 ± 8.6
AUC food intake (a.u.)	134.3 ±2 3.8	97.4 ± 17.9
Glucose (mg/dL)	100.1 ± 4.8	101.6 ± 5.1
Insulin (ng/mL)	0.12 ± 0.01	0.13 ± 0.02
Triglycerides (mg/dL)	53.0 ± 14.4	60.6 ± 8.0
Cholesterol (mg/dL)	77.1 ± 5.0	75.2 ± 4.5
HDL (mg/dL)	40.8 ± 4.2	28.2* ± 1.6
LDL (mg/dL)	26.6 ± 2.1	40.1* ± 3.7
VLDL (mg/dL)	13.1 ± 3.1	14.4 ± 2.7
Castelli index I	2.0 ± 0.12	2.7* ± 0.23
Castelli index II	0.9 ± 0.11	1.4* ± 0.22

Data are presented as mean ± S.E.M.
*Significant ($P < 0.05$) difference from control animals according to a Student's *t* test.
a.u = area unit, AUC = area under the curve (8 weeks).

Effect of circadian desynchrony on cardiovascular parameters

As presented in Fig. 7, circadian desynchrony did not significantly change the baseline MAP (CTR 104.6±2.1 mmHg vs DSC 102.5±2.3 mmHg; $P=0.515$; Fig. 7A) or HR (CTR 352.0±7.8 bpm vs DSC 358.8±6.4 bpm; $P=0.513$; Fig. 7B) in DSC rats compared to CTR rats. However, the bradycardic index in the DSC group was less than that in the CTR group (CTR −2.8±0.2 bpm/mmHg vs DSC −1.8±0.2 bpm/mmHg; $P<0.05$, Fig. 7C), though the tachycardic index was similar in both groups (CTR −3.1±0.7 bpm/mmHg vs DSC −3.7±0.2 bpm/mmHg; $P=0.511$; Fig. 7D).

Discussion

Our results suggest that circadian desynchrony induced by the T22 protocol promotes the reduction of baroreflex sensitivity. However, MAP and HR remained at baseline levels, meaning that the system could maintain control of cardiovascular homeostasis despite baroreflex impairment. We also observed alterations in some metabolic variables, including hepatic insulin resistance, the reduced expression of hepatic antioxidant enzymes (SOD and CAT) and adrenal gland hypertrophy, despite we do not show high plasma insulin and glucose levels. Interestingly, the locomotor activity of DSC rats was less during the dark phase but greater during the light phase than that of CTR rats. In this study we reproduced the forced internal desynchronization applying the T22, as proposed by Campuzano *et al.* (1998). A symmetric 22-h light–dark cycle caused the forced desynchrony of neuronal oscillators within the SCN, which afforded a genetically and neurologically intact animal model of the chronic internal misalignment of circadian rhythms (de la Iglesia *et al.* 2004, Wotus *et al.* 2013,

https://joe.bioscientifica.com
https://doi.org/10.1530/JOE-19-0026

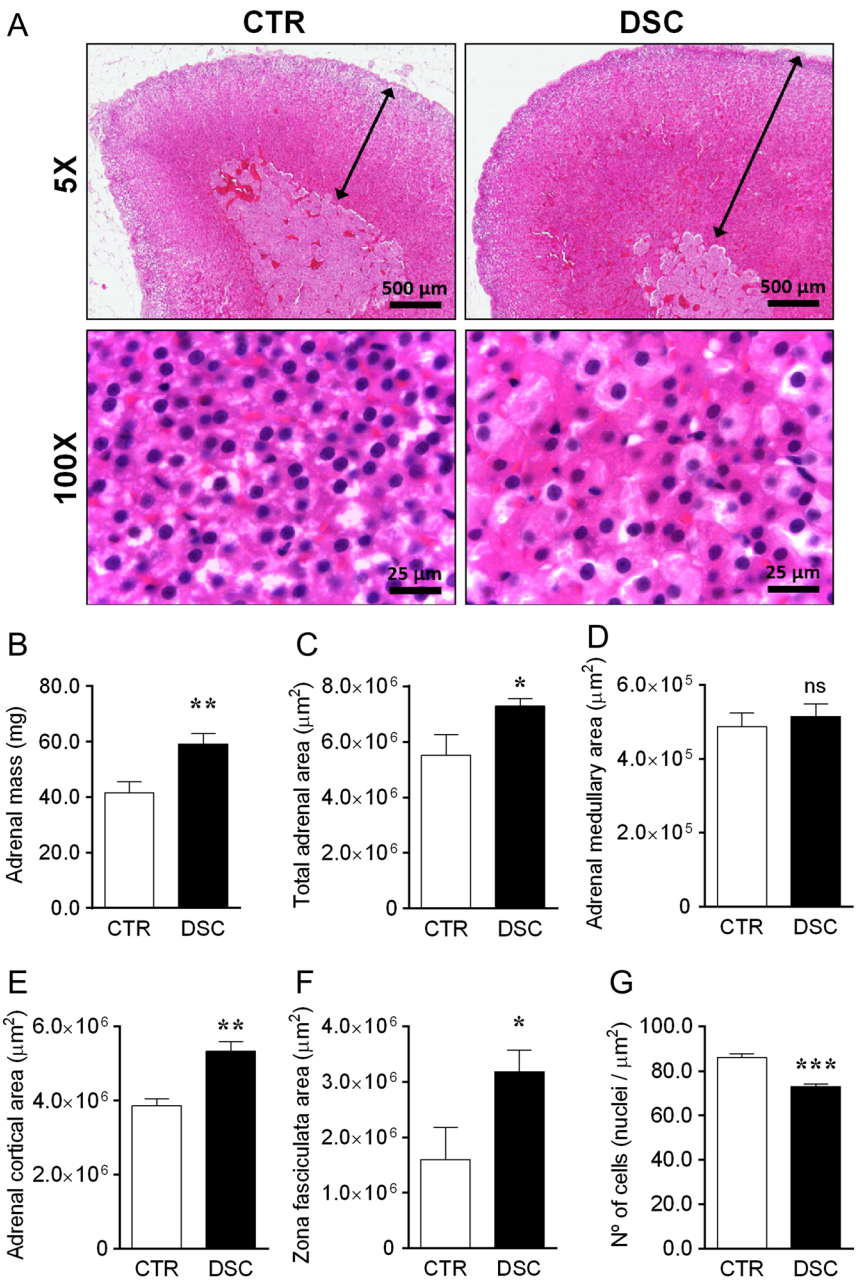

Figure 3
Effect of circadian rhythm desynchronization on adrenal gland morphology. (A) Representative photomicrographs (5× magnification, scale bars = 500 µm and ×100 magnification, scale bars = 25 µm) showing adrenal gland sections stained with hematoxylin–eosin from control (CTR, left) and desynchronized (DSC, right) rats. Adrenal gland mass and total, cortical and zona fasciculata area increased in DSC rats compared to controls (B, C, E and F, respectively). DSC rats showing reduced number of nuclei per µm² in the zona fasciculata of the adrenal cortex (G). Although adrenal medullary area did not differ between the groups (D). Data are presented as mean ± S.E.M. ($n = 6$ each group). *$P < 0.05$ indicates a significant difference from CTR rats according to an unpaired Student's t test. A full colour version of this figure is available at https://doi.org/10.1530/JOE-19-0026.

Ben-Hamo *et al.* 2016). Under T22, rats dissociate the rhythm of locomotor activity into two distinct components: a rhythm synchronized to the light–dark cycle of 22 h and another component with period greater than 24 h which is dissociated from the LD cycle. Because these activity rhythms have different periods their activity bouts coincide at some phases, coincidence activity phase (CAP) and are completely out of phase during the non-coincidence activity phase (NCAP). Thus, in this study, these distinct activity rhythms chronically lead to a state circadian disruption.

Information from the internal and external environment causes the SCN to run on time and prepares the body for subsequent daily tasks. In the absence of SCN activity, however, cortisol and glucose levels do not rise before the beginning of the active period, and BP does not immerse in inactive period of the day (Dallman *et al.* 2004). In normal conditions, a narrow range of variation in BP allows adequate tissue perfusion. In both normal and uncommon physiological situations, several substances in the body interact in complex ways to adjust BP and thereby maintain homeostasis, mediated by the

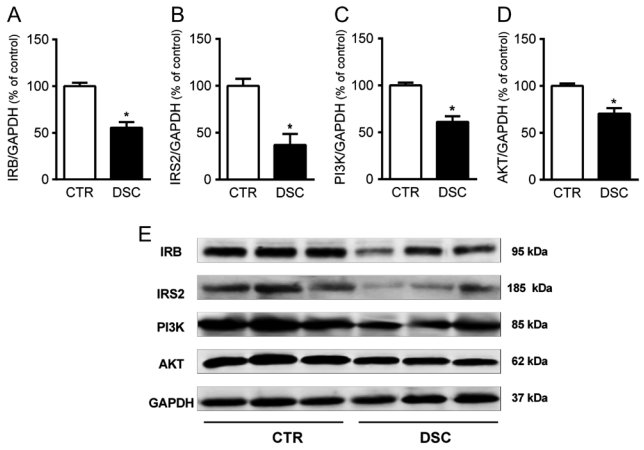

Figure 4
Effect of circadian rhythm desynchronization on insulin signaling proteins in rat livers. (A) Western blot analysis revealing fewer IRB (A), IRS2 (B), PI3K (C) and AKT (D) proteins in desynchronized (DSC) rats than in control (CTR) rats. (E) Representative blots of proteins. GAPDH content was used as control loading. Results are expressed as relative (%) to CTR rats and as mean ± S.E.M. ($n = 6$). *$P < 0.05$ indicates a significant difference from CTR rats according to an unpaired Student's t test.

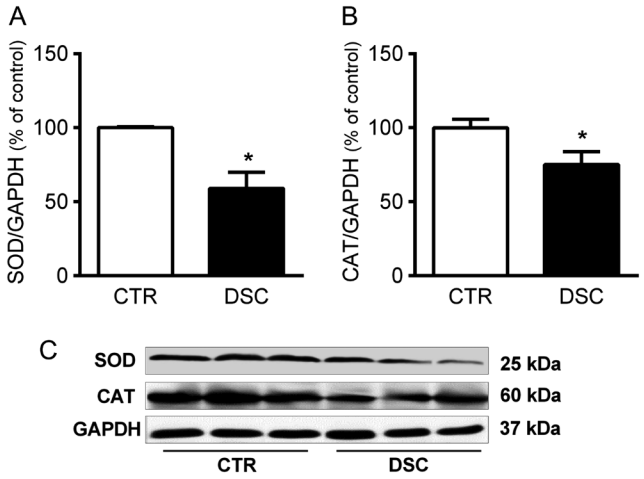

Figure 6
Effect of circadian rhythm desynchronization on antioxidant defense proteins in rat livers. (A) Reduced SOD (A) and CAT (B) among desynchronized (DSC) rats. (C) Representative Western blot of SOD and CAT from the control (CTR) and DSC rats. GAPDH content was used as control loading. Results are expressed as relative (%) to CTR rats and as mean ± S.E.M. ($n = 6$). *$P < 0.05$ indicates a significant difference from CTR rats according to an unpaired Student's t test.

autonomic nervous system and dependent on neural reflexes primarily integrated into the brainstem (Guyenet 2006). In our study, we demonstrated that rats subjected to the T22 protocol for 60 days did not show altered normal baseline levels of MAP and HR. It has been known that baseline values of arterial pressure are determined by the complex interaction of neuroendocrine mechanisms, including arterial compliance, a product of cardiac output by vascular resistance, that directly or indirectly act upon both the amount volume of blood volume pumped by the heart to peripheral tissues. Changes in any of those variables can cause cardiovascular system impairment; however, shifts in alteration in baseline levels of MAP and HR can be offset by counteracting hemodynamic response mechanisms in order to maintain normal levels.

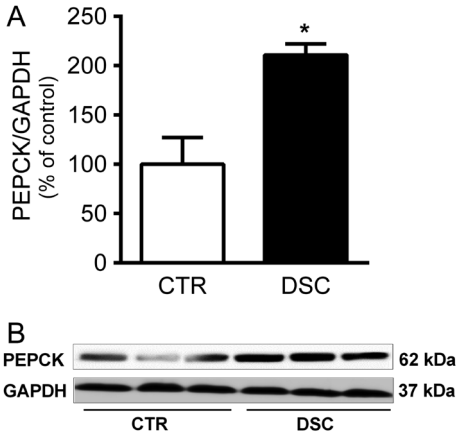

Figure 5
Effect of circadian rhythm desynchronization on gluconeogenic enzyme protein in rat livers. (A) Western blot quantitative analysis showing increased PEPCK protein in desynchronized (DSC) rats. (B) Representative blots of proteins. GAPDH content was used as control loading. Results are expressed as relative (%) to the control group and as mean ± S.E.M. ($n = 6$). *$P < 0.05$ indicates a significant difference from CTR rats according to an unpaired Student's t test.

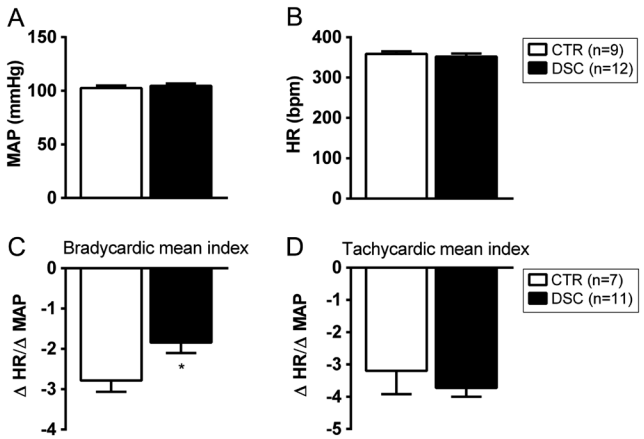

Figure 7
Effect of circadian rhythm desynchronization on cardiovascular parameters. (A) Similar levels of baseline mean arterial pressure (MAP) and (B) heart rate (HR) in rats in the control (CTR, white bars) and desynchronized (DSC, black bars) groups. (C) The DSC rats show reduced baroreflex sensibility expressed as a bradycardic mean index induced by phenylephrine infusion. (D) The tachycardia mean index induced by sodium nitroprusside did not differ between groups. Results are expressed mean ± S.E.M. *$P < 0.05$ indicates a significant difference from CTR rats according to an unpaired Student's t test.

https://joe.bioscientifica.com
https://doi.org/10.1530/JOE-19-0026

However, the bradycardia reflex induced by a vasoconstrictor agent (phenylephrine) is harmed in the DSC animals. In other words, the baroreflex sensitivity is reduced. Several factors can influence the gain and the effectiveness of the baroreflex and its dysfunction affects the cardiovascular variability. The baroreflex sensitivity is a great measure of autonomic cardiac function (Pinna *et al.* 2015). The baroreceptor reflex in this study was induced by intravenous bolus injections of different doses of phenylephrine as a vasopressor agent or sodium nitroprusside as a vasodilator agent and previously described (Moreira *et al.* 2014). The contributions of the sympathetic and parasympathetic components in the compensation of cardiac chronotropic responses are quite distinct in the face of an increase or decrease in blood pressure. The baroreflex tachycardia is determined by the actions of autonomic components, parasympathetic withdrawal and especially greater sympathetic activation, whereas the baroreflex bradycardia is practically determined by vagal activation once sympathetic activity is slow to rapidly compensate increase on arterial pressure (Farah *et al.* 1999). In our study, DSC rats showed a lower bradycardic index than CTR rats, whereas the tachycardia index did not differ between them. Less sensitivity to responses to bradycardia could suggest lower vagal activation in the heart in response to vasoconstriction induced by phenylephrine in desynchronized animals. Otherwise, an attenuated response of reflex bradycardia can be attributed to a reduction in the vagal efferent component of the heart, which suggests an autonomic cardiac imbalance under stressful stimuli. Buijs *et al.* (2014) have shown that the SCN is integral to the neural circuit responsible for the autonomic control of arterial pressure, in which the projections from the solitary tract nucleus (STN) to SCN are essential for this control. Therefore, animals with internal desynchronization could have a dysfunction in the SCN that impairs its running on time and capacity to prepare the body for tasks that promote increases in BP.

In our study, we also observed that animals subjected to the T22 protocol had adrenal gland hypertrophy. Although we did not measure plasma corticosterone levels, others have observed metabolic alterations such as dyslipidemia and energy metabolism in animal models of circadian desynchrony (Aoki *et al.* 2014, West *et al.* 2017), suggesting that liver circadian clock is important to regulate fuel nutrient. In addition, in other study we showed that rats subjected to intrauterine growth restriction have hypercorticosteronemia and adrenal gland hypertrophy (De Oliveira *et al.* 2016). The unregulated release of glucocorticoids negatively affects metabolism by stimulating hepatic and adipose lipogenic activity as well as VLDL secretion and by lowering insulin sensitivity (Chimin *et al.* 2014). In our study reported here, we detected significant dyslipidemia marked by high LDL and low HDL cholesterol along with higher Castelli indexes I and II in DSC rats, which could suggest an increased risk of atherogenesis (Fagundes *et al.* 2009).

We evaluated the hepatic insulin pathway in terms of the expression of IRB, IRS2, PI3K and AKT proteins, which circadian desynchrony induced by the T22 protocol reduced it in the liver. Those results indicate hepatic insulin resistance, which can cause dyslipidemia and increase hepatic gluconeogenesis. In fact, sterol regulatory element-binding transcription factor 1 (SREBP1c) regulates genes required for glucose metabolism, as well as fatty acid and lipid production, while SREBP1c expression is regulated by insulin (Ferré & Foufelle 2010). Insulin signaling suppresses hepatic glucose production by regulating hepatic gluconeogenesis by way of PEPCK expression's ability to coordinate the liver's metabolic response to food intake. Milanski *et al.* (2012) observed hepatic insulin resistance with decreased IRB, pIRS, AKT and pFOXO1 expression in obese animals, though they also detected an increased amount of PEPCK and G6Pase, which suggests an increase in hepatic gluconeogenesis. In our study, we did not detect alterations in fasting glycemia or insulin in DSC rats compared to CTR ones. However, we did find that hepatic insulin resistance increased PEPCK content in the liver, which can cause abnormal glucose metabolism over time. Desynchronized rats in this study showed a greater locomotor activity during light phase (inactivity phase), suggesting probably loss of phase relationship between feeding behavior and hormonal release. Chronically, this would be the hidden mechanism underlying the abnormal hepatic function reported here.

Kohsaka *et al.* (2007) showed that mice fed a high-fat diet present several changes in the diurnal pattern of the expression of lipogenic genes, including a shift in the peak of SREBP1c expression from the dark to the light phase, which suggests that hepatic circadian-clock gene expression changes in male mice fed a high-fat diet.

Other researchers have shown that increased oxidative stress is involved in the pathogenesis of hypertension, dyslipidemia and liver steatosis (Roberts & Sindhu 2009). Oxidative stress can occur as a result of increased ROS production or the failure of the antioxidant system, if not both. The antioxidant system comprises crucial

https://joe.bioscientifica.com
https://doi.org/10.1530/JOE-19-0026

antioxidant enzymes, including SOD and CAT, and the impairment of oxidative defenses in DSC rats can be identified by the lower content of SOD and CAT in the liver. Oxidative stress plays a key role in initiating and advancing nonalcoholic fatty liver disease. In contrast, ROS causes lipid peroxidation, followed by inflammatory responses, and evidence shows that impairment in redox regulation and circadian rhythms can lead to metabolic disorders (Wilking *et al.* 2013, Mindikoglu *et al.* 2017).

Overall, our data indicate that chronic circadian disruption by internal forced desynchronization in rats is a sound animal model to investigate cardiometabolic diseases. In addition, although hypertension was not present after a long period of desynchronization, risk factors such as cardiac autonomic imbalance along with dyslipidemia and hepatic insulin resistance can encourage cardiometabolic disruptions. Such results support the idea that circadian desynchrony, common in night shift work, is likely to be a risk factor of diseases such as diabetes and hypertension. We thus propose that the dissociation of SCN activity induced by the T22 protocol prompts the internal desynchronization of hormonal release and behaviors such as food intake and locomotor activity, which can pose cardiometabolic implications. Further studies using the T22 protocol, however, are needed to determine insulin resistance in other structures such as muscle and adipose tissue, as well as whether cardiometabolic effects can be prevented in desynchronized animals whose food intake is restricted to the active dark phase of the light–dark cycle.

Declaration of interest
The authors declare that there is no conflict of interest that could be perceived as prejudicing the impartiality of the research reported.

Funding
This work was supported by Fundação de Amparo à Pesquisa do Estado de Goiás (FAPEG-201210267001075/005-2012) and Conselho Nacional de Desenvolvimento Científico e Tecnológico (CNPq-449320/2014-6), neither of which was involved in the design, data collection or data analysis of the study, nor in the decision to publish or prepare the manuscript.

Author contribution statement
I G B O designed and conducted the experiments and analyzed the data. M D F J, P R L, D B T C and F A F conducted experiments, while M L F N, E H R S, P C F M, B D V K, C H C, A H F O and G R P analyzed data and interpreted the results of the experiments. R M G and D A R conceived the project, designed the experiments, analyzed the data and wrote, edited and revised the manuscript.

Acknowledgments
The authors thank Dr John Fontenele Araújo at Federal University of Rio Grande do Norte-UFRN, Natal, RN Brazil for providing how to make the wooden cabinets used to study the circadian rhythms of locomotor activity and Dr Marconi Camara Rodrigues of UFRN for his steadfast, selfless technical support in configuring and installing SAP-LNRB software.

References

Alibhai FJ, Tsimakouridze EV, Reitz CJ, Pyle WG & Martino TA 2015 Consequences of circadian and sleep disturbances for the cardiovascular system. *Canadian Journal of Cardiology* **31** 860–872. (https://doi.org/10.1016/j.cjca.2015.01.015)

Alibhai FJ, LaMarre J, Reitz CJ, Tsimakouridze EV, Kroetsch JT, Bolz SS, Shulman A, Steinberg S, Burris TP, Oudit GY, *et al.* 2017 Disrupting the key circadian regulator CLOCK leads to age-dependent cardiovascular disease. *Journal of Molecular and Cellular Cardiology* **105** 24–37. (https://doi.org/10.1016/j.yjmcc.2017.01.008)

Aoki N, Yoshida D, Ishikawa R, Ando M, Nakamura K, Tahara Y & Shibata S 2014 A single daily meal at the beginning of the active or inactive period inhibits food deprivation-induced fatty liver in mice. *Nutrition Research* **34** 613–622. (https://doi.org/10.1016/j.nutres.2014.06.004)

Báez-Ruiz A, Guerrero-Vargas NN, Cázarez-Márquez F, Sabath E, Basualdo MDC, Salgado-Delgado R, Escobar C & Buijs RM 2017 Food in synchrony with melatonin and corticosterone relieves constant light disturbed metabolism. *Journal of Endocrinology* **235** 167–178. (https://doi.org/10.1530/JOE-17-0370)

Bedrosian TA, Fonken LK & Nelson RJ 2016 Endocrine effects of circadian disruption. *Annual Review of Physiology* **78** 109–131. (https://doi.org/10.1146/annurev-physiol-021115-105102)

Ben-Hamo M, Larson TA, Duge LS, Sikkema C, Wilkinson CW, de la Iglesia HO & González MMC 2016 Circadian forced desynchrony of the master clock leads to phenotypic manifestation of depression in rats. *eNeuro* **3** ENEURO.0237-16.2016. (https://doi.org/10.1523/ENEURO.0237-16.2016)

Bray MS, Shaw CA, Moore MWS, Garcia RAP, Zanquetta MM, Durgan DJ, Jeong WJ, Tsai JY, Bugger H, Zhang D, *et al.* 2008 Disruption of the circadian clock within the cardiomyocyte influences myocardial contractile function, metabolism, and gene expression. *American Journal of Physiology: Heart and Circulatory Physiology* **294** H1036–H1047. (https://doi.org/10.1152/ajpheart.01291.2007)

Buijs FN, Cazarez F, Basualdo MC, Scheer FAJL, Perusquía M, Centurion D & Buijs RM 2014 The suprachiasmatic nucleus is part of a neural feedback circuit adapting blood pressure response. *Neuroscience* **266** 197–207. (https://doi.org/10.1016/j.neuroscience.2014.02.018)

Cambras T, Weller JR, Angles-Pujoras M, Lee ML, Christopher A, Diez-Noguera A, Krueger JM & de la Iglesia HO 2007 Circadian desynchronization of core body temperature and sleep stages in the rat. *PNAS* **104** 7634–7639. (https://doi.org/10.1073/pnas.0702424104)

Campuzano A, Vilaplana J, Cambras T & Díez-Noguera A 1998 Dissociation of the rat motor activity rhythm under T-cycles shorter than 24 hours. *Physiology and Behavior* **63** 171–176. (https://doi.org/10.1016/S0031-9384(97)00416-2)

Casiraghi LP, Oda GA, Chiesa JJ, Friesen WO & Golombek DA 2012 Forced desynchronization of activity rhythms in a model of chronic jet lag in mice. *Journal of Biological Rhythms* **27** 59–69. (https://doi.org/10.1177/0748730411429447)

Casiraghi LP, Alzamendi A, Giovambattista A, Chiesa JJ & Golombek DA 2016 Effects of chronic forced circadian desynchronization on body weight and metabolism in male mice. *Physiological Reports* **4** 1–12. (https://doi.org/10.14814/phy2.12743)

Chimin P, Farias Tda S, Torres-Leal FL, Bolsoni-Lopes A, Campaña AB, Andreotti S & Lima FB 2014 Chronic glucocorticoid treatment

enhances lipogenic activity in visceral adipocytes of male Wistar rats. *Acta Physiologica* **211** 409–420. (https://doi.org/10.1111/apha.12226)
Coomans CP, Ramkisoensing A & Meijer JH 2015 The suprachiasmatic nuclei as a seasonal clock. *Frontiers in Neuroendocrinology* **37** 29–42. (https://doi.org/10.1016/j.yfrne.2014.11.002)
Cudney LE, Sassi RB, Behr GA, Streiner DL, Minuzzi L, Moreira JCF & Frey BN 2014 Alterations in circadian rhythms are associated with increased lipid peroxidation in females with bipolar disorder. *International Journal of Neuropsychopharmacology* **17** 715–722. (https://doi.org/10.1017/S1461145713001740)
Dallman MF, Akana SF, Strack AM, Scribner KS, Pecoraro N, La Fleur SE, Houshyar H & Gomez F 2004 Chronic stress-induced effects of corticosterone on brain: direct and indirect. *Annals of the New York Academy of Sciences* **1018** 141–150. (https://doi.org/10.1196/annals.1296.017)
de la Iglesia HO, Cambras T, Schwartz WJ & Díez-Noguera A 2004 Forced desynchronization of dual circadian oscillators within the rat suprachiasmatic nucleus. *Current Biology* **14** 796–800. (https://doi.org/10.1016/j.cub.2004.04.034)
de Oliveira JC, Gomes RM, Miranda RA, Barella LF, Malta A, Martins IP, Franco CC, Pavanello A, Torrezan R, Natali MR, *et al.* 2016 Protein restriction during the last third of pregnancy malprograms the neuroendocrine axes to induce metabolic syndrome in adult male rat offspring. *Endocrinology* **157** 1799–1812. (https://doi.org/10.1210/en.2015-1883)
de Oliveira JC, de Moura EG, Miranda RA, de Moraes AMP, Barella LF, da Conceição EPS, Gomes RM, Ribeiro TA, Malta A, Martins IP, *et al.* 2018 Low-protein diet in puberty impairs testosterone output and energy metabolism in male rats. *Journal of Endocrinology* **237** 243–254. (https://doi.org/10.1530/JOE-17-0606)
Denniff M, Turrell HE, Vanezis A & Rodrigo GC 2014 The time-of-day variation in vascular smooth muscle contractility depends on a nitric oxide signalling pathway. *Journal of Molecular and Cellular Cardiology* **66** 133–140. (https://doi.org/10.1016/j.yjmcc.2013.11.009)
Diez-Noguera A, Vilaplana J, Campuzano A & Cambras T 1994 Presence of two circadian components in the motor activity rhythm of young rats entrained to different T cycles. *Biological Rhythm Research* **25** 181–185. (https://doi.org/10.1080/09291019409360286)
Fagundes ATS, Moura EG, Passos MCF, Santos-Silva AP, De Oliveira E, Trevenzoli IH, Casimiro-Lopes G, Nogueira-Neto JF & Lisboa PC 2009 Temporal evaluation of body composition, glucose homeostasis and lipid profile of male rats programmed by maternal protein restriction during lactation. *Hormone and Metabolic Research* **41** 866–873. (https://doi.org/10.1055/s-0029-1233457)
Farah VM, Moreira ED, Pires MD, Irigoyen MC & Krieger EM 1999 Comparison of three methods for the determination of baroreflex sensitivity in conscious rats. *Brazilian Journal of Medical and Biological Research* **32** 361–369. (https://doi.org/10.1590/S0100-879X1999000300018)
Ferré P & Foufelle F 2010 Hepatic steatosis: a role for de novo lipogenesis and the transcription factor SREBP-1c. *Diabetes, Obesity and Metabolism* **12** 83–92. (https://doi.org/10.1111/j.1463-1326.2010.01275.x)
Gachon F, Nagoshi E, Brown SA, Ripperger J & Schibler U 2004 The mammalian circadian timing system: from gene expression to physiology. *Chromosoma* **113** 103–112. (https://doi.org/10.1007/s00412-004-0296-2)
Gekakis N, Staknis D, Nguyen HB, Davis FC, Wilsbacher LD, King DP, Takahashi JS & Weitz CJ 1998 Role of the CLOCK protein in the mammalian circadian mechanism. *Science* **280** 1564–1569. (https://doi.org/10.1126/science.280.5369.1564)
Golombek DA, Casiraghi LP, Agostino PV, Paladino N, Duhart JM, Plano SA & Chiesa JJ 2013 The times they're a-changing: effects of circadian desynchronization on physiology and disease. *Journal of Physiology* **107** 310–322. (https://doi.org/10.1016/j.jphysparis.2013.03.007)
Gómez-Abellán P, Hernández-Morante JJ, Luján JA, Madrid JA & Garaulet M 2008 Clock genes are implicated in the human metabolic syndrome. *International Journal of Obesity* **32** 121–128. (https://doi.org/10.1038/sj.ijo.0803689)
Guyenet PG 2006 The sympathetic control of blood pressure. *Nature Reviews: Neuroscience* **7** 335–346. (https://doi.org/10.1038/nrn1902)
Inouye S-ITS & Kawamura H 1979 Persistence of circadian rhythmicity in a mammalian hypotalamic 'island' containing the suprachiasmatic nucleus. *PNAS* **76** 5962–5966. (https://doi.org/10.1073/pnas.76.11.5962)
Kalsbeek A, van der Spek R, Lei J, Endert E, Buijs RM & Fliers E 2012 Circadian rhythms in the hypothalamo-pituitary-adrenal (HPA) axis. *Molecular and Cellular Endocrinology* **349** 20–29. (https://doi.org/10.1016/j.mce.2011.06.042)
Karatsoreos IN, Bhagat S, Bloss EB, Morrison JH & McEwen BS 2011 Disruption of circadian clocks has ramifications for metabolism, brain, and behavior. *PNAS* **108** 1657–1662. (https://doi.org/10.1073/pnas.1018375108)
King DP, Zhao Y, Sangoram AM, Wilsbacher LD, Tanaka M, Antoch MP, Steeves TD, Vitaterna MH, Kornhauser JM, Lowrey PL, *et al.* 1997 Positional cloning of the mouse circadian clock gene. *Cell* **89** 641–653. (https://doi.org/10.1016/S0092-8674(00)80245-7)
Kingsbury NJ, Taylor SR & Henson MA 2016 Inhibitory and excitatory networks balance cell coupling in the suprachiasmatic nucleus: a modeling approach. *Journal of Theoretical Biology* **397** 135–144. (https://doi.org/10.1016/j.jtbi.2016.02.039)
Kohsaka A, Laposky AD, Ramsey KM, Estrada C, Joshu C, Kobayashi Y, Turek FW & Bass J 2007 High-fat diet disrupts behavioral and molecular circadian rhythms in mice. *Cell Metabolism* **6** 414–421. (https://doi.org/10.1016/j.cmet.2007.09.006)
Laing EE, Johnston JD, Möller-Levet CS, Bucca G, Smith CP, Dijk DJ & Archer SN 2015 Exploiting human and mouse transcriptomic data: identification of circadian genes and pathways influencing health. *BioEssays* **37** 544–556. (https://doi.org/10.1002/bies.201400193)
Milanski M, Arruda AP, Coope A, Ignacio-Souza LM, Nunez CE, Roman EA, Romanatto T, Pascoal LB, Caricilli AM, Torsoni MA, *et al.* 2012 Inhibition of hypothalamic inflammation reverses diet-induced insulin resistance in the liver. *Diabetes* **61** 1455–1462. (https://doi.org/10.2337/db11-0390)
Mindikoglu AL, Opekun AR, Gagan SK & Devaraj S 2017 Impact of time-restricted feeding and dawn-to-sunset fasting on circadian rhythm, obesity, metabolic syndrome, and nonalcoholic fatty liver disease. *Gastroenterology Research and Practice* **2017** 3932491. (https://doi.org/10.1155/2017/3932491)
Mohawk JA & Takahashi JS 2011 Cell autonomy and synchrony of suprachiasmatic nucleus circadian oscillators. *Trends in Neurosciences* **34** 349–358. (https://doi.org/10.1016/j.tins.2011.05.003)
Moreira MCS, Da Silva EF, Silveira LL, De Paiva YB, De Castro CH, Freiria-Oliveira AH, Rosa DA, Ferreira PM, Xavier CH, Colombari E, *et al.* 2014 High sodium intake during postnatal phases induces an increase in arterial blood pressure in adult rats. *British Journal of Nutrition* **112** 1923–1932. (https://doi.org/10.1017/S0007114514002918)
Morris CJ, Yang JN & Scheer FA 2012 The impact of the circadian timing system on cardiovascular and metabolic function. *Progress in Brain Research* **199** 337–358. (https://doi.org/10.1016/B978-0-444-59427-3.00019-8)
Morris CJ, Purvis TE, Hu K & Scheer FAJL 2016 Circadian misalignment increases cardiovascular disease risk factors in humans. *PNAS* **113** E1402–E1411. (https://doi.org/10.1073/pnas.1516953113)
Morris CJ, Purvis TE, Mistretta J, Hu KScheer FAJL 2018 Circadian misalignment increases C-reactive protein and blood pressure in chronic shift workers. *Journal of Biological Rhythms* **32** 154–164. (https://doi.org/10.1177/0748730417697537)
Oike H, Sakurai M, Ippoushi K & Kobori M 2015 Time-fixed feeding prevents obesity induced by chronic advances of light/dark cycles in mouse models of jet-lag/shift work. *Biochemical and Biophysical*

Research Communications **465** 556–561. (https://doi.org/10.1016/J.BBRC.2015.08.059)

Pezuk P, Mohawk JA, Yoshikawa T, Sellix MT & Menaker M 2010 Circadian organization is governed by extra-SCN pacemakers. *Journal of Biological Rhythms* **25** 432–441. (https://doi.org/10.1177/0748730410385204)

Pinna GD, Maestri R & La Rovere MT 2015 Assessment of baroreflex sensitivity from spontaneous oscillations of blood pressure and heart rate: proven clinical value? *Physiological Measurement* **36** 741–753. (https://doi.org/10.1088/0967-3334/36/4/741)

Podobed P, Pyle WG, Ackloo S, Alibhai FJ, Tsimakouridze EV, Ratcliffe WF, Mackay A, Simpson J, Wright DC, Kirby GM, *et al.* 2014 The day/night proteome in the murine heart. *American Journal of Physiology: Regulatory, Integrative and Comparative Physiology* **307** R121–R137. (https://doi.org/10.1152/ajpregu.00011.2014)

Portaluppi F 2014 The circadian organization of the cardiovascular system in health and disease. *Indian Journal of Experimental Biology* **52** 395–398.

Richards J, Cheng KY, All S, Skopis G, Jeffers L, Jeanette Lynch IJ, Wingo CS & Gumz ML 2013 A role for the circadian clock protein Per1 in the regulation of aldosterone levels and renal Na+ retention. *American Journal of Physiology: Renal Physiology* **305** F1697–F1704. (https://doi.org/10.1152/ajprenal.00472.2013)

Roberts CK & Sindhu KK 2009 Oxidative stress and metabolic syndrome. *Life Sciences* **84** 705–712. (https://doi.org/10.1016/j.lfs.2009.02.026)

Scheer FAJL, Hilton MF, Mantzoros CS & Shea SA 2009 Adverse metabolic and cardiovascular consequences of circadian misalignment. *PNAS* **106** 4453–4458. (https://doi.org/10.1073/pnas.0808180106)

Schwartz MD, Wotus C, Liu T, Friesen WO, Borjigin J, Oda GA & de la Iglesia HO 2009 Dissociation of circadian and light inhibition of melatonin release through forced desynchronization in the rat. *PNAS* **106** 17540–17545. (https://doi.org/10.1073/pnas.0906382106)

Scott EM, Carter AM & Grant PJ 2008 Association between polymorphisms in the clock gene, obesity and the metabolic syndrome in man. *International Journal of Obesity* **32** 658–662. (https://doi.org/10.1038/sj.ijo.0803778)

Sokolove PG & Bushell WN 1978 The chi square periodogram: its utility for analysis of circadian rhythms. *Journal of Theoretical Biology* **72** 131–160. (https://doi.org/10.1016/0022-5193(78)90022-x)

Tseng HL, Yang SC, Yang SH & Shieh KR 2015 Hepatic circadian-clock system altered by insulin resistance, diabetes and insulin sensitizer in mice. *PLoS ONE* **10** e0120380. (https://doi.org/10.1371/journal.pone.0120380)

West AC, Smith L, Ray DW, Loudon ASI, Brown TM & Bechtold DA 2017 Misalignment with the external light environment drives metabolic and cardiac dysfunction. *Nature Communications* **8** 417. (https://doi.org/10.1038/s41467-017-00462-2)

Wilking M, Ndiaye M, Mukhtar H & Ahmad N 2013 Circadian rhythm connections to oxidative stress: implications for human health. *Antioxidants and Redox Signaling* **19** 192–208. (https://doi.org/10.1089/ars.2012.4889)

Wotus C, Lilley TR, Neal AS, Suleiman NL, Schmuck SC, Smarr BL, Fischer BJ & de la Iglesia HO 2013 Forced desynchrony revels independent contributions of suprachiasmatic oscillators to the daily plasma corticosterone rhythm in male rats. *PLoS ONE* **8** 1–12. (https://doi.org/10.1371/journal.pone.0068793)

Received in final form 10 April 2019
Accepted 9 May 2019
Accepted Preprint published online 9 May 2019